Inorg. Chem. **2002**, *41*, 1383–1390

Nickel Complexes of Bidentate [S_2] and [SN] Borato Ligands

Pinghua Ge, Arnold L. Rheingold, and Charles G. Riordan*

Department of Chemistry and Biochemistry, University of Delaware, Newark, Delaware 19716

Received September 12, 2001

Nickel(II) complexes of the monoanionic borato ligands [$Ph_2B(CH_2SCH_3)_2$] (abbreviated Ph_2Bt), [$Ph_2B(CH_2S^tBu)_2$] (Ph_2Bt^{tBu}), [Ph_2B(1-pyrazolyl)(CH_2SCH_3)], and [Ph_2B(1-pyrazolyl)(CH_2S^tBu)] have been prepared and characterized. While [Ph_2Bt] formed the square planar homoleptic complex, $[Ph_2Bt]_2Ni$, the larger [S_2] ligand with *tert*-butyl substituents, [Ph_2Bt^{tBu}], yielded an unexpected organometallic derivative, $[Ph_2Bt^{tBu}]Ni(\eta^2\text{-}CH_2SBu^t)$, resulting from B–C bond rupture. The analogous thiametallacycle derived from the [S_3] ligand, [$PhB(CH_2S^tBu)_3$] ($PhTt^{tBu}$), has been structurally authenticated (Schebler, P. J.; Mandimutsira, B. S.; Riordan, C. G.; Liable-Sands, L.; Incarvito, C. D.; Rheingold, A. L. *J. Am. Chem. Soc.* **2001**, *123*, 331). The [SN] borato ligands formed exclusively the cis stereoisomers upon reaction with Ni(II) sources, $[Ph_2B$(1-pyrazolyl)$(CH_2SR)]_2Ni$. Analysis of the Ni(II/I) reduction potentials by cyclic voltammetry revealed a ~600 mV anodic shift upon replacement of two thioether donors ($[Ph_2Bt]_2Ni$) with two pyrazolyl donors ($[Ph_2B$(1-pyrazolyl)$(CH_2SCH_3)]_2Ni$) consistent with the all thioether environment stabilizing the lower oxidation state of nickel.

Introduction

Our laboratory has been interested in the coordination chemistry of tridentate borato ligands, [$PhTt^R$] and [$Ph(pz^{R'})Bt^R$], which present [S_3] or [S_2N] donors, respectively, to metal ions, Chart 1.[1−6] The ligand design permits stereoelectronic control of resulting metal complexes by appropriate choice of the substituents on sulfur and/or the pyrazolyl ring. To date, we have prepared [$PhTt^R$] derivatives where the sulfur substituent R is methyl, phenyl, *para*-tolyl, *iso*-propyl, or *tert*-butyl. The first three ligands yield complexes of the form $[PhTt^R]_2M$ where two ligands are accommodated at a single metal ion.[2] Alternatively, the [$PhTt^{iPr}$] and [$PhTt^{tBu}$] ligands, because of the larger size of the sulfur substituents, promote formation of [$PhTt^R$]MX complexes.[7] The latter species are ripe for further synthetic elaboration at the M−X unit. Similar steric control is achieved in the mixed donor [S_2N] ligands, [Ph(pz)Bt^R]. For example, [Ph(pz)Bt] forms the derivative, *cis*-$[Ph(pz)Bt]_2Ni$, whereas [$Ph(pz^{tBu})Bt^{tBu}$] yields monomeric [$Ph(pz^{tBu})Bt^{tBu}$]NiCl. In the case of a ligand of intermediate bulk, [Ph(pz)Bt^{tBu}], the resulting nickel complex is the five coordinate, chloride-bridged dimer, $\{[Ph(pz)Bt^{tBu}]NiCl\}_2$, in the solid state while monomeric in solution.[8]

Beyond the aforementioned coordination chemistry observations, current applications of these ligands include the preparation of functional models for mononuclear zinc enzyme active sites,[9] the development the nickel, cobalt, and iron organometallic chemistry,[10] and nickel-promoted dioxygen activation[11] supported by these thioether-rich ligands. With respect to organometallic transformations, we have demonstrated that the $B-CH_2$ bonds of [$PhTt^{tBu}$] are susceptible to cleavage under certain conditions. For example, reaction of [$PhTt^{tBu}$]NiCl with CH_3Li produced the novel thiametallacycle, $[\kappa^2\text{-}PhTt^{tBu}]Ni(\eta^2\text{-}CH_2SBu^t)$, via such a ligand degradation pathway.[10] Mechanistic studies confirmed that the thiametallacycle arises from alkylation of [$PhTt^{tBu}$]NiCl by excess borato ligand generated during the reaction. To date, this represents the only example of instability of the [$PhTt^R$] ligands.

* To whom correspondence should be addressed. E-mail: riordan@udel.edu.

(1) Ge, P.; Riordan, C. G.; Haggerty, B. S.; Rheingold, A. L. *J. Am. Chem. Soc.* **1994**, *116*, 8406−8407.
(2) Ohrenberg, C.; Ge, P.; Schebler, P.; Riordan, C. G.; Yap, G. P. A.; Rheingold, A. L. *Inorg. Chem.* **1996**, *35*, 749−754.
(3) Ohrenberg, C.; Riordan, C. G.; Liable-Sands, L.; Rheingold, A. L. *Coord. Chem. Rev.* **1998**, *174*, 301−311.
(4) Schebler, P.; Riordan, C. G.; Liable-Sands, L.; Rheingold, A. L. *Inorg. Chim. Acta* **1998**, *270*, 543−549.
(5) Chiou, S.-J.; Ge, P.; Riordan, C. G.; Liable-Sands, L.; Rheingold, A. L. *Chem. Commun.* **1999**, 159−160.
(6) Ohrenberg, C.; Riordan, C. G.; Liable-Sands, L. M.; Rheingold, A. L. *Inorg. Chem.* **2001**, *40*, 4276−4283.
(7) Schebler, P. J.; Riordan, C. G.; Guzei, I.; Rheingold, A. L. *Inorg. Chem.* **1998**, *37*, 4754−4755.
(8) Chiou, S.-J.; Riordan, C. G. Unpublished results.
(9) Chiou, S.-J.; Innocent, J.; Lam, K.-C.; Riordan, C. G.; Liable-Sands, L.; Rheingold, A. L. *Inorg. Chem.* **2000**, *39*, 4347−4353.
(10) Schebler, P. J.; Mandimutsira, B. S.; Riordan, C. G.; Liable-Sands, L.; Incarvito, C. D.; Rheingold, A. L. *J. Am. Chem. Soc.* **2001**, *123*, 331−332.
(11) Mandimutsira, B. S.; Yamarik, J. L.; Brunold, T. C.; Gu, W.; Cramer, S. P.; Riordan, C. G. *J. Am. Chem. Soc.* **2001**, *123*, 9194−9195.

10.1021/ic010966r CCC: $22.00
Published on Web 02/16/2002

Chart 1

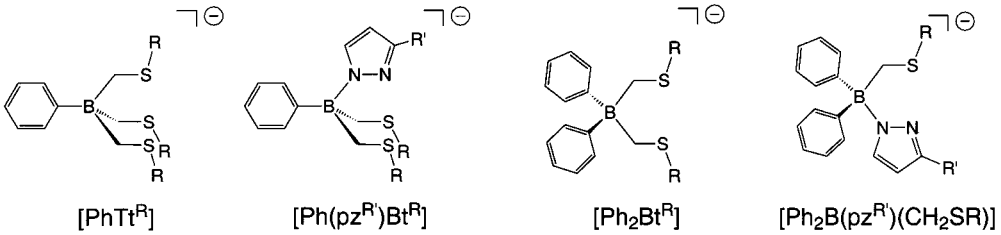

Concurrent with our studies of the tridentate ligands, we have been developing synthetic strategies for the corresponding bidentate borato ligands, $[Ph_2Bt^R]$ and $[Ph_2B(pz^R)(CH_2SR)]$, Chart 1.[5,12] As anionic ligands, comparison can be made to related monoanionic, bidentate ligands such as bis(pyrazolyl)borates, β-diketonates, and the recently popularized β-diketiminates.[13] Herein, we report the preparation, characterization, and comparative electrochemical properties of nickel complexes of the borato ligands $[Ph_2Bt]$, $[Ph_2Bt^{tBu}]$, $[Ph_2B(pz)(CH_2SCH_3)]$, and $[Ph_2B(pz)(CH_2S(CH_2SBu^t)]$. The preparations of $[Ph_2Bt]_2Ni$ and $[Ph_2B(pz)(CH_2SCH_3)]_2Ni$ have been communicated.[5,12]

Results and Discussion

Ligand Syntheses. The $[S_2]$ ligands, $[Ph_2Bt]$ and $[Ph_2Bt^{tBu}]$, were prepared conveniently following protocols developed in this laboratory for the tridentate ligands, $[PhTt^R]$.[6] The requisite sulfide, CH_3SR ($R = CH_3$, Bu^t), was readily and quantitatively deprotonated by *n*-BuLi in the presence of TMEDA. The resulting carbanion, $LiCH_2SR$, was added slowly to Ph_2BBr yielding the desired product. Aqueous workup with either $[Bu_4N]Br$ or CsCl as the cation source yielded the ligands, $[Bu_4N]Ph_2Bt$ and $[Cs]Ph_2Bt^{tBu}$, as air-stable, microcrystalline white solids in moderate yields (45−80%). The reactivity and properties of the ligand prepared with either countercation were indistinguishable. The salts are soluble in chlorinated hydrocarbons, THF, and acetone. Complete spectroscopic data are contained in the Experimental Section.

The [SN] borato ligands, containing one thioether and one pyrazolyl donor, were prepared using a stepwise, in situ procedure. Addition of equimolar $LiCH_2SR$ ($R = CH_3$, Bu^t) to Ph_2BBr at −78 °C in THF effected the incorporation of one thioether substituent to the borane. The presumed product, $Li[Ph_2B(Br)(CH_2SR)]$, was not isolated; however, its formation was inferred from the identity of the final [SN] product. To the THF solution was introduced 1 equiv of Lipz. The resulting mixture was stirred for 12 h, after which time the desired ligand was precipitated in yields of 40−65% by addition of aqueous $[Bu_4N]Br$. The white solids, $[Bu_4N][Ph_2B(pz)(CH_2SCH_3)]$ and $[Bu_4N][Ph_2B(pz)(CH_2SBu^t)]$, are soluble in chlorinated hydrocarbons, THF, and acetone. Complete spectroscopic data are contained in the Experimental Section. The direct preparation of the [SN] ligands by sequential introduction of the thioether and pyrazolyl groups is convenient and highly reproducible. Provided the introduction of the $LiCH_2SR$ is conducted at low temperature, there is no evidence for the formation of either of the undesired $[S_2]$ or $[N_2]$ borato ligands. Similar preparative approaches have led to the isolation of the analogous $[S_2N]$ borato ligands, $[Ph(pz^R)Bt^{R'}]$.

Preparation of Metal Complexes. The synthesis of the square planar nickel complexes is outlined in Scheme 1. Each complex was accessible from either $NiCl_2 \cdot 6\ H_2O$ or $Ni(BF_4)_2 \cdot 6\ H_2O$ and 2 molar equiv of the corresponding ligand salt in methanol. The resulting red solids were diamagnetic as judged by their sharp ^1H NMR resonances, and therefore, each species possesses a square planar structure. $[Ph_2Bt]_2Ni$, $[Ph_2B(pz)(CH_2SCH_3)]_2Ni$, and $[Ph_2B(pz)(CH_2SBu^t)]_2Ni$ are stable and highly soluble in a range of noncoordinating organic solvents including chlorinated hydrocarbons, acetone, benzene, and nitromethane. For the two complexes derived from the [SN] ligands, $[Ph_2B(pz)(CH_2SCH_3)]_2Ni$ and $[Ph_2B(pz)(CH_2SBu^t)]_2Ni$, cis and trans isomers are possible. Proton NMR spectra of these complexes displayed a single set of resonances in accord with either the existence of a single isomer or facile equilibration (on the NMR time scale) between isomers. Low-temperature spectra are consistent with the former interpretation. That is, $[Ph_2B(pz)(CH_2SCH_3)]_2Ni$ and $[Ph_2B(pz)(CH_2SBu^t)]_2Ni$ are present as single isomers. Each is assigned as the cis structure on the basis of the following considerations. The bis$[S_2N]$ analogues of nickel, cobalt, and iron, $[Ph(pz)Bt]_2M$, for which the molecular structures have been elucidated, exist solely as the cis isomers.[5] This observation suggests an electronic preference for pyrazolyl substituents to reside trans to the thioether, rather than trans to another pyrazolyl group. A similar electronic preference should persist in $[Ph_2B(pz)(CH_2SCH_3)]_2Ni$ favoring the cis form. While in the absence of a crystal structure this analysis is reasonable for $[Ph_2B(pz)(CH_2SCH_3)]_2Ni$, it might not appear as satisfying for $[Ph_2B(pz)(CH_2SBu^t)]_2Ni$ in which the cis isomer would necessarily place two *tert*-butyl thioether donors in adjacent coordination sites. However, careful inspection of X-ray structures of the related complexes $[Ph_2Bt]_2Ni$ and $[Ph_2Bt]_2Pd$[14] show that the sulfur substituents are projected in roughly orthogonal directions. That is, one S−C vector lies in the metal's coordination plane, while the other is perpendicular to the metal's plane. Consequently, van der Waals' contacts between adjacent *tert*-butyl thioether groups in $[Ph_2B(pz)(CH_2SBu^t)]_2Ni$ should be minimal. On the basis of these considerations and the present lack of crystals suitable for X-ray analysis, we are left to

(12) Ge, P.; Riordan, C. G.; Yap, G. P. A.; Rheingold, A. L. *Inorg. Chem.* **1996**, *35*, 5408−5409.

(13) For one recent example: Kim, W. K.; Fevola, M. J.; Liable-Sands, L. M.; Rheingold, A. L.; Theopold, K. H. *Organometallics* **1998**, *17*, 4541−4543.

(14) Schebler, P. J.; Rheingold, A. L.; Riordan, C. G. Unpublished results.

Scheme 1

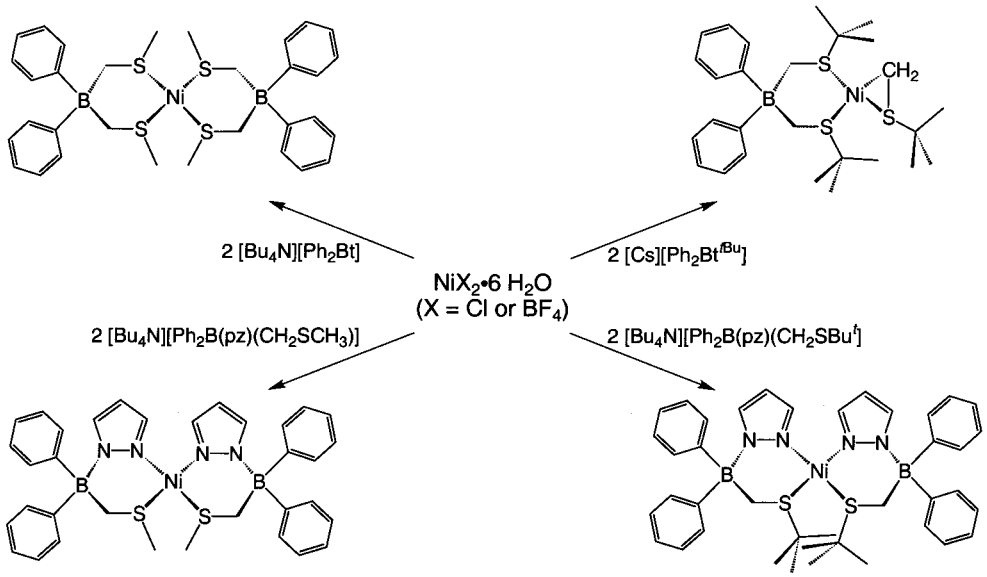

Scheme 2

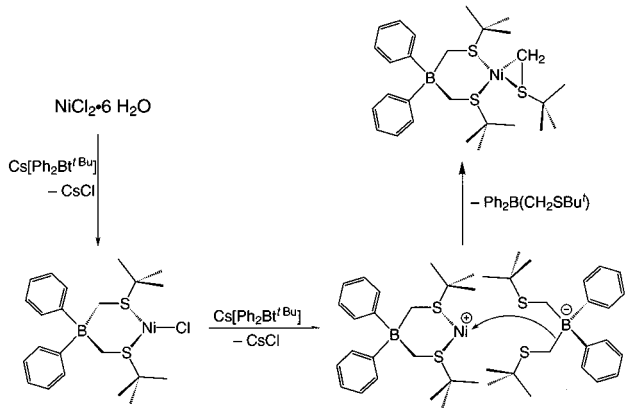

propose $[Ph_2B(pz)(CH_2SCH_3)]_2Ni$ and $[Ph_2B(pz)(CH_2S(CH_3)_3)]_2Ni$ form the cis isomers exclusively.

Reaction of 2 equiv of $Cs[Ph_2Bt^{tBu}]$ with $NiCl_2$ generated a single, diamagnetic product in high yield (76%), Scheme 1. In stark contrast with the preparation of $[Ph_2Bt]_2Ni$, the material generated was not the simple homoleptic complex, $[Ph_2Bt^{tBu}]_2Ni$. Rather, the nickel thiametallacycle, $[Ph_2Bt^{tBu}]Ni(\eta^2\text{-}CH_2SBu^t)$, was produced. The species contains one $[Ph_2Bt^{tBu}]$ borato ligand and an alkyl thioether derived from degradation of the second equivalent of $[Ph_2Bt^{tBu}]$. The tridentate ligand, $[PhTt^{tBu}]$, reacts analogously with $NiCl_2$ yielding $[\kappa^2\text{-}PhTt^{tBu}]Ni(\eta^2\text{-}CH_2SBu^t)$, in which the borato ligand is bound through two sulfurs.[10] Alternatively, reduction of $[PhTt^{tBu}]NiCl$ generates $[\kappa^2\text{-}PhTt^{tBu}]Ni(\eta^2\text{-}CH_2SBu^t)$ in approximately 40% yield. In the latter reaction, the proposed reduction results in the release of free borato ligand which subsequently alkylates $[PhTt^{tBu}]NiCl$. The proposed mechanism for formation of $[Ph_2Bt^{tBu}]Ni(\eta^2\text{-}CH_2SBu^t)$ is contained in Scheme 2. Coordination of one $[Ph_2Bt^{tBu}]$ results in a three-coordinate $[Ph_2Bt^{tBu}]NiCl$.[15] This 14-electron intermediate should be sufficiently electrophilic to be alkylated by $[Ph_2Bt^{tBu}]$. Alternatively, the two-coordinate nickel complex generated by chloride abstraction by Cs^+ (as shown in Scheme 2) may be the active electrophile. In either scenario, alkylation yields the thiametallacycle and $Ph_2B(CH_2SBu^t)$.

Molecular Structures. The solid-state structure of $[Ph_2Bt]_2Ni$ is contained in Figure 1 with crystallographic and metric parameters in Tables 1 and 2, respectively. The Ni ion resides on a crystallographic inversion center which renders trans thioethers metrically equivalent and ensures a planar ligation sphere. The Ni−S bond lengths of 2.200(1) and 2.240(1) Å are consistent with previously reported Ni(II)−thioether distances in square planar geometries and are ∼0.1 Å longer than Ni(II)−S(thiolate) bond lengths.[16] The bite angle of the borato ligand is slightly less than 90 °; ∠S(1)−Ni−S(2) = 86.31(4)°. The six-membered chelate ring resides in a twisted boat conformation which orients one of the methyl groups (C(15)) essentially perpendicular to the NiS_4 plane (displacement from S_4 plane, 1.66 Å) while the other (C(16)) lies nearly in the NiS_4 plane (displacement from S_4 plane, 0.11 Å). This disposition of the chelate ring places the phenyl substituents in distinct positions. One (Ph_{eq}) is directed away from the Ni while the other (Ph_{ax}) is located directly above the NiS_4 plane. This latter orientation results in phenyl canopies protecting the open axial coordination sites with the Ph_{ax} centroid−Ni distance of 3.79 Å. A similar placement of pseudoaxial phenyl groups has been noted in the molecular structure of $[Ph_2B(pz)_2]_2Ni$, in which the Ph_{eq} centroid−Ni distance is 3.45 Å.[17] Variable temperature proton NMR studies in CD_2Cl_2 established a facile equilibration of the Ph_{eq} and Ph_{ax} groups in $[Ph_2Bt]_2Ni$ with an activation energy (E_a) of 9 kcal/mol. The proposed mechanism of equilibration entails concerted isomerization of the chelate rings from one twist boat to another as depicted in Scheme 3. The small value of E_a precludes alternative pathways involving Ni−S bond breaking.

(15) An elegant example of three-coordinate Ni(II): Mindiola, D. J.; Hillhouse, G. L. *J. Am. Chem. Soc.* **2001**, *123*, 4623−4624.

(16) Halcrow, M. A.; Christou, G. *Chem. Rev.* **1994**, *94*, 2421−2481.

(17) Cotton, F. A.; Murillo, C. A. *Inorg. Chim. Acta* **1976**, *17*, 121−124.

Table 1. Crystallographic Data for $[Ph_2Bt]_2Ni$, $[Ph_2Bt^{tBu}]Ni(\eta^2\text{-}CH_2SBu^t)$, $[Bu_4N]_2[trans\text{-}(Ph_2Bt)_2NiBr_2]$ and $[Bu_4N]_2[cis\text{-}(Ph_2Bt)_2Ni(NCS)_2]$

	$[Ph_2Bt]_2Ni$	$[Ph_2Bt^{tBu}]Ni(\eta^2\text{-}CH_2SBu^t)$	$[Bu_4N]_2[trans\text{-}(Ph_2Bt)_2NiBr_2]$	$[Bu_4N]_2[cis\text{-}(Ph_2Bt)_2Ni(NCS)_2]$
formula	$C_{32}H_{40}B_2NiS_4$	$C_{27}H_{43}BNiS_3$	$C_{64}H_{112}B_2Br_2N_2NiS_4$	$C_{68}H_{115}B_2N_5NiS_6$
fw	633.21	533.31	781.87	1275.34
space group	$P2_1/n$	$P2_1/n$	$Pna2_1$	$P\bar{1}$
color, habit	orange block	orange blade	green/yellow plate	yellow blade
a, Å	10.3144(9)	9.7472(2)	22.2330(4)	13.42540(10)
b, Å	9.365(2)	15.0844(2)	10.3879(4)	13.6055(2)
c, Å	16.793(1)	19.4406(2)	29.6866(6)	21.8006(2)
α, deg				76.653(1)
β, deg	107.624(9)	94.9262(4)		86.038(1)
γ, deg				76.233(1)
V, Å^3	1546.0(3)	2847.82(6)	6856.2(3)	3762.79(7)
Z,	2	4	4	2
ρ (calcd), g cm^{-3}	1.360	1.244	1.480	1.126
μ(Mo Kα), cm^{-1}	9.19	9.14	16.08	4.64
temp, K	293(2)	173(2)	213(2)	173(2)
diffractometer			Siemens P4/CCD	
radiation			Mo Kα ($\lambda = 0.71073$ Å)	
R(*F*), %[a]	4.04	7.06	4.10	5.49
R(*wF*^{2}), %[a]	8.53	19.08	19.26	14.08

[a] Quantity minimized $= R(wF^2) = \sum[w(F_o^2 - F_c^2)^2]/\sum[(wF_o^2)^2]^{1/2}$; $R = \sum|F_o - F_c|/(F_o) \times 100\%$.

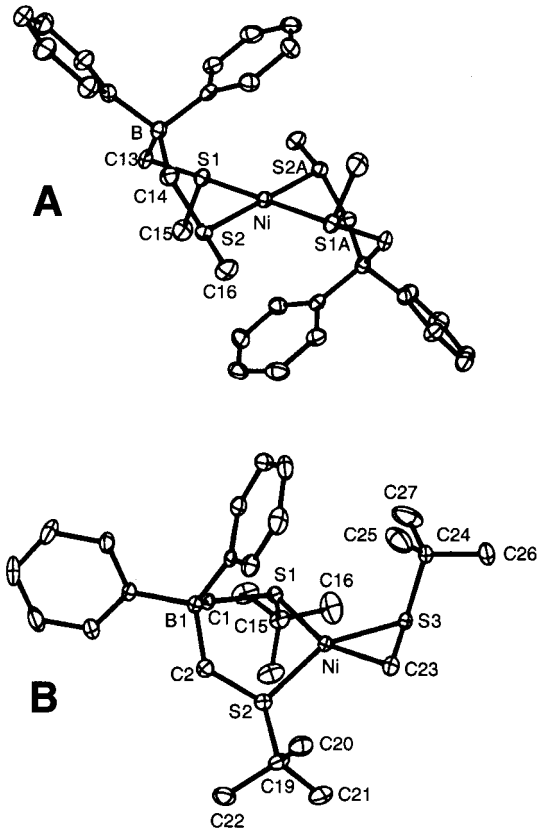

Figure 1. Thermal ellipsoid plots of $[Ph_2Bt]_2Ni$ (A) and $[Ph_2Bt^{tBu}]Ni(\eta^2\text{-}CH_2SBu^t)$ (B) at 30% probability level; hydrogen atoms not shown.

The structure of $[Ph_2Bt^{tBu}]Ni(\eta^2\text{-}CH_2SBu^t)$, shown in Figure 1, highlights the unexpected consequence of positioning *tert*-butyl substituents on the sulfur donors of the bidentate borato ligand, $[Ph_2Bt^R]$. The borato ligand is coordinated in the bidentate mode with the chelate ring in the twist boat conformation. The Ni−S(1) bond distance for the thioether trans to the alkyl group is longer (2.232(2) Å) than the other, mutually trans thioethers Ni−S (2.178(2) and 2.149(2) Å) because of the trans influence of the alkyl substituent. The Ni−C(23) bond distance is 1.926(5) Å. Expectedly, the Ni−S−C angle of the metallacycle is acute at 58.5(2)°. The solid-state structure shows a slight twist from square planar, 14°, a consequence of close contact between the phenyl substituent of the borato ligand and the *tert*-butyl of the alkyl thioether fragment. Metric parameters agree well

Table 2. Selected Bond Lengths (Å) and Bond Angles (deg) for $[Ph_2Bt]_2Ni$, $[Ph_2Bt^{tBu}]Ni(\eta^2\text{-}CH_2SBu^t)$, $[Bu_4N]_2[trans\text{-}(Ph_2Bt)_2NiBr_2]$, and $[Bu_4N]_2[cis\text{-}(Ph_2Bt)_2Ni(NCS)_2]$

	$[Ph_2Bt]_2Ni$		
Ni−S(1)	2.244(1)	S(1A)−Ni−S(2)	93.69(4)
Ni−S(2)	2.200(1)	C(15)−S(1)−C(13)	101.8(2)
S(1)−C(15)	1.799(4)	C(15)−S(1)−Ni	107.3(2)
S(1)−C(13)	1.818(4)	C(13)−S(1)−Ni	111.2(2)
S(2)−C(16)	1.806(4)	C(16)−S(2)−C(14)	101.0(2)
S(2)−C(14)	1.808(4)	C(16)−S(2)−Ni	116.0(2)
S(1)−Ni−S(2)	86.31(4)	C(14)−S(2)−Ni	106.3(1)
	$[Ph_2Bt^{tBu}]Ni(\eta^2\text{-}CH_2SBu^t)$		
Ni−C(23)	1.926(5)	S(3)−Ni−S(1)	108.70(7)
Ni−S(1)	2.232(2)	S(2)−Ni−S(1)	95.59(7)
Ni−S(2)	2.178(2)	C(1)−S(1)−C(15)	105.0(3)
Ni−S(3)	2.148(2)	C(1)−S(1)−Ni	110.0(2)
C(23)−Ni−S(3)	49.6(1)	C(15)−S(1)−Ni	109.3(3)
C(23)−Ni−S(2)	107.2(1)	C(2)−S(2)−Ni	109.5(2)
S(3)−Ni−S(2)	152.79(8)	C(23)−S(3)−Ni	58.5(2)
C(23)−Ni−S(1)	157.2(1)	C(24)−S(3)−Ni	113.9(2)
	$[Bu_4N]_2[trans\text{-}(Ph_2Bt)_2NiBr_2]$		
Ni−S(2)	2.470(2)	S(1)−Ni−S(4)	178.40(7)
Ni−S(3)	2.470(2)	S(2)−Ni−Br(1)	88.68(5)
Ni−S(1)	2.476(2)	S(3)−Ni−Br(1)	88.81(5)
Ni−S(4)	2.476(2)	S(1)−Ni−Br(1)	89.41(5)
Ni−Br(1)	2.591(1)	S(4)−Ni−Br(1)	92.13(5)
Ni−Br(2)	2.625(1)	S(2)−Ni−Br(2)	91.21(5)
S(2)−Ni−S(3)	176.98(7)	S(3)−Ni−Br(2)	91.32(5)
S(2)−Ni−S(1)	88.70(7)	S(1)−Ni−Br(2)	89.65(5)
S(3)−Ni−S(1)	92.95(7)	S(4)−Ni−Br(2)	88.81(5)
S(2)−Ni−S(4)	90.87(6)	S(1)−Ni−S(4)	178.40(7)
S(3)−Ni−S(4)	87.55(7)		
	$[Bu_4N]_2[cis\text{-}(Ph_2Bt)_2Ni(NCS)_2]$		
Ni−N(2)	2.041(3)	N(2)−Ni−S(2)	177.7(1)
Ni−N(1)	2.049(3)	N(1)−Ni−S(2)	88.7(1)
Ni−S(1)	2.451(1)	S(1)−Ni−S(2)	91.38(3)
Ni−S(3)	2.462(1)	S(3)−Ni−S(2)	90.91(3)
Ni−S(2)	2.470(1)	N(2)−Ni−S(4)	87.8(1)
Ni−S(4)	2.486(1)	N(1)−Ni−S(4)	177.8(1)
N(2)−Ni−N(1)	93.6(1)	S(1)−Ni−S(4)	89.90(3)
N(2)−Ni−S(1)	88.9(1)	S(3)−Ni−S(4)	89.29(3)
N(1)−Ni−S(1)	91.9(1)	S(2)−Ni−S(4)	89.92(3)
N(2)−Ni−S(3)	88.8(1)	C(33)−N(1)−Ni	153.2(3)
N(1)−Ni−S(3)	88.9(1)	C(34)−N(2)−Ni	167.7(3)
S(1)−Ni−S(3)	177.57(4)		

Scheme 3

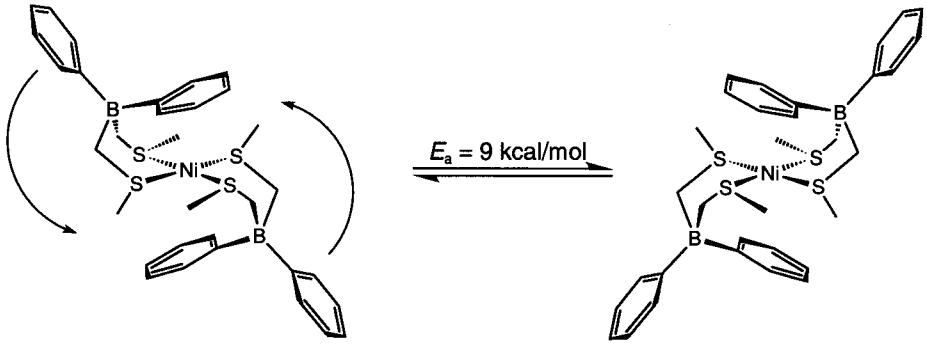

Table 3. Cyclic Voltammetry Data for $[Ph_2Bt]_2Ni$, $[Ph_2B(pz)(CH_2SCH_3)]_2Ni$, $[Ph_2B(pz)(CH_2SBu^t)]_2Ni$, and $[Bp^*]_2Ni$

cmpd	E_f,[a] V	ΔE_p, mV	$I_{p,a}/I_{p,c}$	
$[Ph_2Bt]_2Ni$	−1.13	140	0.92	quasireversible
$[Ph_2B(pz)(CH_2SCH_3)]_2Ni$	−1.69			irreversible
$[Ph_2B(pz)(CH_2SBu^t)]_2Ni$	−1.73			irreversible
$[Bp^*]_2Ni$[28]	−2.42			irreversible

[a] Vs Fc/Fc^+ in CH_2Cl_2.

with those determined for the related complex, $[\kappa^2$-$PhTt^{tBu}]$-$Ni(\eta^2$-$CH_2SBu^t)$, prepared similarly.[10] The latter complex contains the potentially tridentate borato ligand coordinated via only two thioethers. Related η^2-CH_2SCH_3 ligated complexes of nickel have been reported, for example, (PPh_3)-$Ni(Cl)(\eta^2$-$CH_2SCH_3)$,[18] although this report represents the first nickel derivative to be structurally authenticated. Cationic $[(PPh_3)_2Pd(\eta^2$-$CH_2SCH_3)]^+$ and neutral $[Cp_2Ti(PMe_3)$-$(\eta^2$-$CH_2SCH_3)]$ are selected examples from either end of the transition series for which molecular structures have been determined.[19,20] The C(23)—S(3) bond distance of 1.720(5) Å in $[Ph_2Bt^{tBu}]Ni(\eta^2$-$CH_2SBu^t)$ is midway between that of a C—S single bond (1.82 Å) and a C═S double bond (1.61 Å), suggesting some contribution from resonance structure **B**, the methylene *tert*-butylsulfonium ion, should be considered.

Bond valence analysis of $[Ph_2Bt^{tBu}]Ni(\eta^2$-$CH_2SBu^t)$ yields a C—S bond order of 1.24 in agreement with substantial double bond character and in accord with contribution from resonance form **B**.[21]

Electrochemical Properties. Cyclic voltammetry data for $[Ph_2Bt]_2Ni$, $[Ph_2B(pz)(CH_2SCH_3)]_2Ni$, $[Ph_2B(pz)(CH_2SBu^t)]_2$-Ni, and $[Bp^*]_2Ni$ (Bp*, dihydrobis(3,5-dimethylpyrazolyl)-borate) in CH_2Cl_2 are contained in Table 3. Formal potentials are referenced to Fc/Fc^+. Each complex displays a cathodic wave at negative potentials assigned to the Ni(II)/Ni(I) couple. No anodic peaks were noted up to 1.2 V. Comparison of the reductive peak currents with internal ferrocene corroborates the assignment of one-electron processes. Only $[Ph_2Bt]_2Ni$ shows a quasireversible signal at modest scan velocities (<1 V/s). The other three complexes are reduced irreversibly on the electrochemical time scale in scan rate dependent processes. The trend in reduction potentials supports the propensity with which thioethers stabilize the lower valent states of nickel.[22] That is, the $Ni[S_4]$ complex, $[Ph_2Bt]_2Ni$, has the most accessible Ni(I) state at −1.13 V. The two $Ni[S_2N_2]$ complexes are reduced at similar potentials which are ~600 mV more negative than those for $[Ph_2Bt]_2Ni$. The complex with the least polarizable ligands, $[Bp^*]_2Ni$, is the most difficult of the four to reduce with a potential of less than −2.4 V. The assignment of the cathodic waves to Ni(I) formation is supported by chemical reduction of $[Ph_2$-$Bt]_2Ni$ with Na/Hg. The resulting pale yellow material, Na-$[(Ph_2Bt)_2Ni]$, has been characterized as an authentic Ni(I) complex on the basis of its rhombic ESR signal (g = 2.27, 2.17, 2.09) and its Ni L-edge X-ray absorption spectrum.[23] The integrated intensity of the latter is diagnostic for assigning the nickel oxidation state. Recently, we have demonstrated that reduction of $[PhTt^{tBu}]NiCl$ ($E_{1/2}$ = −1.30 mV) in the presence of suitable donor ligands (CO, CNR, PMe_3) generates isolable T_d Ni(I) derivatives, $[PhTt^{tBu}]Ni$-(L).[10]

Reactivity of $[Ph_2Bt]_2Ni$. The ligand substitution chemistry of square planar $[Ph_2Bt]_2Ni$ is summarized in Scheme 4. Brick red $[Ph_2Bt]_2Ni$ dissolved in CH_3CN to form a yellowish-green solution with optical characteristics in accord with six-coordinate nickel formulated as $[Ph_2Bt]_2Ni(CH_3$-$CN)_2$; d—d transitions occur at 593 and 940 nm. Formation is reversible as solvent removal under vacuum generates the red starting material. Similar observations made in pyridine are suggestive of reversible $[Ph_2Bt]_2Ni(py)_2$ production. $[Ph_2$-$Bt]_2Ni$ reacts with 2 molar equiv of $[Bu_4N]Br$ to form yellow-green $[Bu_4N]_2[trans$-$(Ph_2Bt)_2NiBr_2]$. The molecular structure has been established by X-ray diffraction, Figure 2, with selected metric parameters in Table 2. To accommodate the axial bromide donors, the two borato chelate rings adopt twist chair conformations which place the phenyl groups away

(18) Davidson, J. G.; Barefield, E. K.; VanDerveer, D. G. *Organometallics* **1985**, *4*, 1178−1184.
(19) Miki, K.; Kai, Y.; Yasuoka, N.; Kasai, N. *Bull. Chem. Soc. Jpn.* **1981**, *54*, 3639−3647.
(20) Park, J. W.; Henling, L. M.; Schaefer, W. P.; Grubbs, R. H. *Organometallics* **1990**, *9*, 1650−1656.
(21) Thorp, H. H. *Inorg. Chem.* **1992**, *31*, 1585−1588.
(22) Musie, G.; Reibenspies, J. H.; Darensbourg, M. Y. *Inorg. Chem.* **1998**, *37*, 302−310.
(23) Wang, H.; Ge, P.; Riordan, C. G.; Brooker, S.; Woomer, C. G.; Collins, T.; Balasubramanian, M.; Melendres, C.; Graudejus, O.; Bartlett, N.; Cramer, S. P. *J. Phys. Chem.* **1998**, *102*, 8343−8346.

Scheme 4

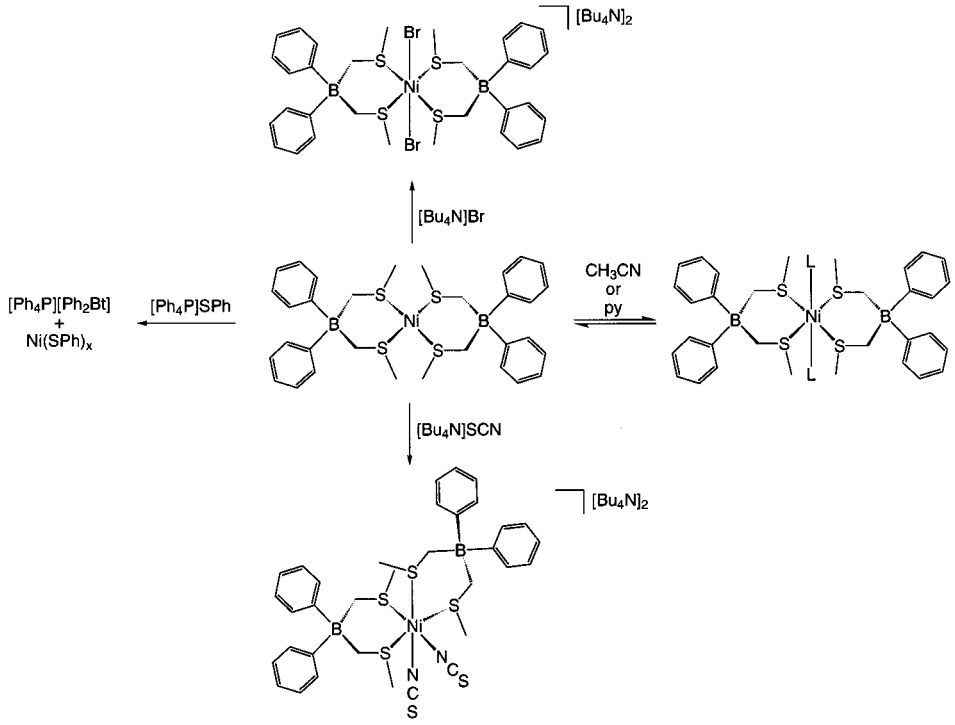

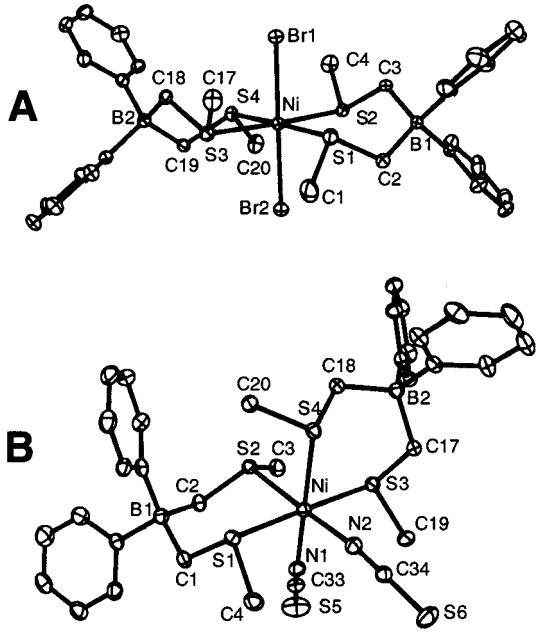

Figure 2. Thermal ellipsoid plots of anions of $[Bu_4N]_2$[*trans*-$(Ph_2Bt)_2NiBr_2$] (A) and $[Bu_4N]_2$[*cis*-$(Ph_2Bt)_2Ni(NCS)_2$] (B) at 30% probability level; hydrogen atoms not shown.

from the nickel. Consequently, the Ni−B distance increases from 3.41 to 4.13 Å. The structure is metrically similar to neutral *trans*-$(MeSCH_2CH_2SMe)_2NiBr_2$.[24] In the anion, the Ni−S bond lengths are similar with an average distance of 2.47 Å, 0.25 Å longer than in the four coordinate precursor.

Addition of excess $[Bu_4N]SCN$ to $[Ph_2Bt]_2Ni$ in THF yields $[Bu_4N]_2$[*cis*-$(Ph_2Bt)_2Ni(NCS)_2$] as a blue crystalline solid. Two equal intensity ν_{CN} vibrations are present in the IR spectrum at 2090 and 2084 cm^{-1} supporting the cis stereochemistry. The similar intensities of the symmetric and asymmetric vibrational modes indicate orthogonal thiocyanate vectors.[25] In contrast, the trans isomer would have a very weak or unobservable symmetric ν_{CN} mode (IR forbidden). The structure of $[Bu_4N]_2$[*cis*-$(Ph_2Bt)_2Ni(NCS)_2$] is depicted in Figure 2. The thiocyanates are coordinated via nitrogen with Ni−N−C angles of 167.7° and 153.2 °. The Ni−S bonds trans to the thiocyanates are slightly longer, 2.47 and 2.49 Å, than the mutually trans Ni−S thioethers, 2.45 and 2.46 Å. The borato ligands are bound in different conformations. As in $[Bu_4N]_2$[*trans*-$(Ph_2Bt)_2NiBr_2$], the chelate rings have opened from the twist boat configuration of $[Ph_2Bt]_2Ni$ to accommodate two additional ligands. One is in a chair, and the other, a twist chair orientation. Perhaps the most unusual aspect of the structure is the cis stereochemistry. As described above, $[Bu_4N]_2$[*trans*-$(Ph_2Bt)_2NiBr_2$] exists as the trans isomer. Furthermore, the neutral analogue, $(MeSCH_2CH_2SMe)_2Ni(NCS)_2$, forms exclusively the trans isomer.[24] The isomeric preference may be energetically small, although the trans form of $[Bu_4N]_2$[*cis*-$(Ph_2Bt)_2Ni(NCS)_2$] has not been detected. In the cis isomer, the N-bound thiocyanates occupy positions trans to the soft thioether ligands rather than mutually trans. This may be the source of the preference for the cis isomer.

Summary

Bidentate borato ligands possessing two thioether donors [S_2] and one thioether, one pyrazole donor [SN] are synthetically accessible in multigram quantities. Nickel complexes of four such ligands have been prepared and fully character-

(24) Kockerling, M.; Henkel, G. *Z. Naturforsch., B: Chem. Sci.* **1996**, *51*, 178−186.

(25) Cotton, F. A.; Wilkinson, G. In *Advanced Inorganic Chemistry*, 4th ed.; John Wiley & Sons: New York, 1988; p 1036−1037.

ized. For the [S_2] ligands, the sulfur substituent impacts greatly product formation. [Ph_2Bt] yields the homoleptic complex, [$Ph_2Bt]_2Ni$, which reacts further with bromide or thiocyanate to form the corresponding six-coordinate species. Alternatively, [Ph_2Bt^{tBu}] does not generate the homoleptic complex. Rather, [Ph_2Bt^{tBu}]Ni(η^2-CH_2SBu^t) is formed via borato ligand B−C bond cleavage: a reaction that is promoted to reduce steric congestion at nickel. Formation of the thiametallacycle is the outcome of other nickel-based reactions including reduction of [$PhTt^{tBu}$]NiCl. Electrochemical analysis of a series of neutral, square planar Ni(II) complexes highlights the propensity with which the thioether donors stabilize the Ni(I) state. $[Ph_2Bt]_2Ni$ is reduced at a potential 1.2 V more accessible than that of $[Bp^*]_2Ni$ with the mixed [SN] donor complexes, $[Ph_2B(pz)(CH_2SCH_3)]_2$-Ni and $[Ph_2B(pz)(CH_2SBu^t)]_2Ni$, exhibiting reductions midway between these two extremes.

Experimental Section

Materials and Methods. Unless otherwise stated, all reagents were obtained from commercial sources and used without further purification. When dry solvents were required, they were distilled under N_2 and dried as indicated. Hexanes, Et_2O, THF, toluene, benzene, and pentanes were freshly distilled over Na/benzophenone. Acetonitrile, CH_2Cl_2, pyridine, and TMEDA were distilled over CaH_2, the latter two under reduced pressure. HPLC grade acetone (≤0.05% H_2O) and benzonitrile (≤0.005% H_2O) were purchased from Acros Organics, Fisher Scientific. HPLC grade acetonitrile (≤0.001% H_2O) was purchased from Burdick and Jackson, Inc. Ph_2BBr,[26] Bu^tSCH_3,[27] and $[Bu_4N]Ph_2Bt$[12] were prepared according to procedures previously outlined in the literature. All ligands and metal complexes were dried under vacuum at refluxing acetone temperatures unless otherwise stated. Elemental analyses were performed by Desert Analytics, Inc., Tuscon, AZ. Electronic spectra were recorded with a Hewlett-Packard 8453 diode array spectrophotometer. NMR spectra were recorded on a 400 MHz Brüker spectrometer equipped with a Sun workstation, a Brüker AM-250, or a Brüker AC-250 spectrometer. Samples were referenced to the residual protio solvent signal. Cyclic voltammetry was performed on a BAS 50W system. All experiments were performed in an Ar-filled glovebox in a cell consisting of a glassy carbon or platinum disk working electrode (r = 1 mm), Pt wire counter electrode, and Ag/AgCl reference electrode. Solutions contained 0.1 M electrolyte ([Bu_4N][PF_6], dried prior to use) and 10 mM sample. Potentials were referenced to internal Fc/Fc^+ (+410 mV vs Ag/AgCl).

Caution. *$(CH_3)_2S$ is a flammable liquid and presents a pungent odor. The deprotonation reaction should be vented through an aqueous solution of NaOCl.*

Cs[Ph_2Bt^{tBu}]. CH_3SBu^t (2.65 g, 25.4 mmol) and TMEDA (0.1 mL, 0.65 mmol) were charged into a 300-mL flask under a N_2 atmosphere. *n*-BuLi (10 mL, 2.5 M in hexanes) was added dropwise via syringe over 5 min and allowed to stir for 8 h. The solution was cooled to −78 °C and 20 mL of THF added followed by Ph_2-BBr (3.06 g, 12.5 mmol) in 20 mL benzene. The mixture was allowed to warm to 25 °C and stirred for 48 h. The reaction was terminated by addition of 30 mL of H_2O. Volatile organics were removed by rotary evaporation, the aqueous solution was filtered through Celite, and the product precipitated by addition of aqueous CsCl (2.1 g, 12.5 mmol). The white precipitate was isolated by filtration, washed with H_2O (2 × 30 mL), and dried under vacuum. Yield: 2.9 g (46%). ^{1}H NMR (CD_3NO_2): δ 7.38 (br, *m*-C_6H_5, 4 H), 7.01 (t, *o*-C_6H_5, 4 H), 6.85 (t, *p*-C_6H_5, 2 H), 2.13 (q, BCH_2, $^2J_{B-H}$ = 4.5 Hz, 4 H), 1.26 (s, CH_3, 18 H). ^{13}C NMR (CD_3NO_2): δ 135.2 (*m*-C_6H_5), 127.3 (*o*-C_6H_5), 123.7 (*p*-C_6H_5), 40.5 ($C(CH_3)_3$), 31.4 (CH_3), 26.2 (q, BCH_2, $^1J_{B-C}$ = 162 Hz). Anal. Calcd for $C_{22}H_{32}BCsS_2$: C, 52.4%; H, 6.40%. Found: C, 52.0%; H, 6.70%.

[Bu_4N][$Ph_2B(pz)(CH_2SCH_3)$]. $(CH_3)_2S$ (3.5 mL, 47.6 mmol) and TMEDA (0.1 mL, 0.65 mmol) were charged into a 300-mL flask under a N_2 atmosphere. *n*-BuLi (10 mL, 2.5 M in hexanes) was added dropwise via syringe over 5 min and stirred for 1 h. The mixture was heated to 40 °C for 1 h to remove excess $(CH_3)_2S$. The solution was cooled to −78 °C and 30 mL of THF added. This solution was added slowly to Ph_2BBr (6.12 g, 25 mmol) in 30 mL THF. The mixture was allowed to warm to 25 °C and stirred for 1 h. In a separate flask, pyrazole (1.7 g, 25 mmol) was dissolved in 20 mL of THF. Upon cooling to −78 °C, *n*-BuLi (10 mL, 2.5 M in hexanes) was added dropwise via syringe over 5 min. At 25 °C, the Li pyrazolate solution was transferred to the borane solution and stirred for 12 h. The reaction was terminated by addition of 30 mL of H_2O. Volatile organics were removed by rotary evaporation, the aqueous solution was filtered through Celite, and the product precipitated by addition of aqueous [Bu_4N]Br (8.06 g, 25 mmol). The white precipitate was isolated by filtration, washed with H_2O (2 × 30 mL), and dried under vacuum. Yield: 8.6 g (65%). ^{1}H NMR (CD_3NO_2): δ 7.50 (s, pz, 1 H), 7.28 (s, pz, 1 H), 7.24 (d, *m*-C_6H_5, 4 H), 7.03 (t, *o*-C_6H_5, 4 H), 6.93 (t, *p*-C_6H_5, 2 H), 6.00 (s, pz, 1H), 3.25 (t, NCH_2, 8 H), 2.45 (s, BCH_2, 2 H), 1.97 (s, SCH_3, 3 H), 1.72 (p, CH_2, 8 H), 1.41 (h, CH_2, 8 H), 0.98 (t, CH_3, 12 H). ^{13}C NMR (CD_3NO_2): δ 137.0 (pz), 134.1 (pz), 133.2 (*m*-C_6H_5), 126.0 (*o*-C_6H_5), 123.3 (*p*-C_6H_5), 101.5 (pz), 58.0 (NCH_2), 24.0 (CH_2), 20.4 (SCH_3), 19.6 (CH_2), 13.7 (CH_3). Anal. Calcd for $C_{33}H_{54}$-BN_3S: C, 74.0%; H, 10.16%; N, 7.84%. Found: C, 74.0%; H, 10.16%; N, 7.66%.

[Bu_4N][$Ph_2B(pz)(CH_2SBu^t)$]. CH_3SBu^t (2.7, 25.9 mmol) and TMEDA (0.1 mL, 0.65 mmol) were charged into a 300-mL flask under a N_2 atmosphere. *n*-BuLi (10 mL, 2.5 M in hexanes) was added dropwise via syringe over 5 min and allowed to stir for 8 h. The solution was cooled to −78 °C and 30 mL of THF added. This solution was added slowly to Ph_2BBr (6.12 g, 25 mmol) in 30 mL of THF. The mixture was brought to 25 °C and stirred for 1 h. In a separate flask, pyrazole (1.7 g, 25 mmol) was dissolved in 20 mL of THF. Upon cooling to −78 °C, *n*-BuLi (10 mL, 2.5 M in hexanes) was added dropwise via syringe over 5 min. At 25 °C, the Li pyrazolate solution was transferred to the borane solution and stirred for 12 h. The reaction was terminated by addition of 30 mL of H_2O. Volatile organics were removed by rotary evaporation, the aqueous solution was filtered through Celite, and the product precipitated by addition of aqueous [Bu_4N]Br (8.06 g, 25 mmol). The white precipitate was isolated by filtration, washed with H_2O (2 × 30 mL), and dried under vacuum. Yield: 6.2 g (43%). ^{1}H NMR ($CDCl_3$): δ 7.92 (s, pz, 1 H), 7.45 (s, pz, 1 H), 7.35 (d, *m*-C_6H_5, 4 H), 7.06 (t, *o*-C_6H_5, 4 H), 6.95 (t, *p*-C_6H_5, 2 H), 6.14 (s, pz, 1H), 2.51 (t, NCH_2, 8 H), 2.40 (s, BCH_2, 2 H), 1.28 (s, SCH_3, 3 H), 1.22 (m, CH_2, 16 H), 0.93 (t, CH_3, 12 H). ^{13}C NMR (CD_3-NO_2): δ 138.2 (pz), 134.4 (pz), 135.3 (*m*-C_6H_5), 127.1 (*o*-C_6H_5), 124.6 (*p*-C_6H_5), 102.5 (pz), 60.0 (NCH_2), 40.8 ($C(CH_3)_3$), 31.1 (CH_2), 24.8 ($C(CH_3)_3$), 20.7 (CH_2), 13.9 (CH_3). Anal. Calcd for $C_{36}H_{60}BN_3S$: C, 74.8%; H, 10.5%; N, 7.27%. Found: C, 74.8%; H 10.3%; N, 7.27%.

[$Ph_2Bt]_2Ni$. [$Ni(H_2O)_6$](BF_4)$_2$ (500 mg, 1.47 mmol) was dissolved in 50 mL of methanol. To the solution was added solid

(26) Eisch, J.; King, R. B. In *Organometallic Syntheses*; Academic Press: New York, 1981; pp 126−127.
(27) Vogel, A. I.; Cowan, D. M. *J. Chem. Soc.* **1943**, 18.
(28) Kokusen, H.; Sohrin, Y.; Matsui, M.; Hata, Y.; Hasegawa, H. *J. Chem. Soc., Dalton Trans.* **1996**, 195−201.

$[Bu_4N]Ph_2Bt$ (1.56 g, 2.95 mmol) resulting in the slow precipitation of a brick red solid. The red solid was collected via filtration, washed with 10 mL of methanol, and dried in vacuo. Yield: 744 mg (80%). UV−vis (CH_2Cl_2) λ_{max} (ϵ, $M^{-1}cm^{-1}$): 354 nm (7300), 412 nm (7800). ^1H NMR ($CDCl_3$): δ 7.26 (br, *m*-C_6H_5, 8 H), 7.20 (t, *o*-C_6H_5, 8 H), 7.06 (t, *p*-C_6H_5, 4 H), 1.82 (s, CH_2 and CH_3, 20 H). ^{13}C NMR (CD_2Cl_2): δ 133.0 (*m*-C_6H_5), 128.1 (*o*-C_6H_5), 125.0 (*p*-C_6H_5), 22.0 (CH_3). Anal. Calcd for $C_{32}H_{40}B_2S_4Ni$: C, 60.7%; H, 6.37%. Found: C, 60.5%; H, 6.17%.

$[Ph_2Bt^{tBu}]Ni(\eta^2\text{-}CH_2SBu^t)$. Anhydrous $NiCl_2$ (100 mg, 0.77 mmol) was charged into a flask and suspended in 20 mL of THF. $Cs[Ph_2Bt^{tBu}]$ (776 mg, 1.54 mmol) was added as a solid, resulting in a color change to red, yielding a homogeneous solution after 24 h. The solvent was removed under vacuum and the resulting residue dissolved in 10 mL of methylene chloride, filtered, and concentrated to a volume of 2 mL. Slow solvent evaporation yielded red crystals. Yield: 302 mg (76%). Similar yields were obtained using the $[Bu_4N]$ salt of the $[Ph_2Bt^{tBu}]$ ligand. UV−vis (THF) λ_{max} (ϵ, M^{-1} cm^{-1}): 300 nm (4000), 470 nm (400). ^1H NMR (CD_3CN): δ 7.25 (br, *m*-C_6H_5, 4 H), 7.04 (t, *o*-C_6H_5, 4 H), 6.89 (t, *p*-C_6H_5, 2 H), 1.42 (s, $C(CH_3)_3$, 18 H), 1.33 (br m, CH_2, 6 H), 1.13 (s, $C(CH_3)_3$, 9 H). Anal. Calcd for $C_{27}H_{43}BS_3Ni$: C, 60.8%; H, 8.13%. Found: C, 59.7%; H, 7.99%.

$[Ph_2B(pz)(CH_2SCH_3)]_2Ni$. $[Ni(H_2O)_6](BF_4)_2$ (200 mg, 0.59 mmol) was dissolved in 20 mL of methanol. To the solution was added solid $[Bu_4N][Ph_2B(pz)(CH_2SCH_3)]$ (630 mg, 1.18 mmol) resulting in the slow precipitation of a brick red solid. The red solid was collected via filtration, washed with 10 mL methanol, and dried in vacuo. Yield: 243 mg (61%). UV−vis (THF) λ_{max} (ϵ, M^{-1} cm^{-1}): 321 nm (4200), 486 nm (250). ^1H NMR ($CDCl_3$): δ 7.50 (br, pz + C_6H_5, 6 H), 7.19 (m, pz + C_6H_5, 7 H), 6.87 (t, *p*-C_6H_5, 2 H), 6.01 (t, pz, 1 H), 2.04 (d, BCH_2, 2 H), 1.33 (s, SCH_3, 6 H), 1.10 (d, BCH_2, 2 H). Anal. Calcd for $C_{34}H_{36}B_2N_4S_2Ni$: C, 63.3%; H, 5.62%; N, 8.68%. Found: C, 63.1%; H, 5.34%; N, 8.68%.

$[Ph_2B(pz)(CH_2SBu^t)]_2Ni$. $[Ni(H_2O)_6](BF_4)_2$ (200 mg, 0.59 mmol) was dissolved in 20 mL of methanol. To the solution was added solid $[Bu_4N][Ph_2B(pz)(CH_2SBu^t)]$ (680 mg, 1.18 mmol) resulting in the slow precipitation of a brick red solid. The red solid was collected via filtration, washed with 10 mL of methanol, and dried in vacuo. Yield: 232 mg (54%). UV−vis (THF) λ_{max} (ϵ, M^{-1} cm^{-1}): 321 nm (4200), 486 nm (250). ^1H NMR ($CDCl_3$): δ 7.45 (m, pz + C_6H_5, 3 H), 7.33 (d, pz, 2 H), 7.14 (m, *p*-C_6H_5, 4 H), 7.06 (t, pz, 1 H), 6.88 (t, C_6H_5, 2 H), 5.93 (t, pz, 2 H) 1.82 (d, BCH_2, 2 H), 1.43 (d, BCH_2, 1 H), 1.33 (s, $SC(CH_3)_3$, 18 H). Anal. Calcd for $C_{40}H_{48}B_2N_4S_2Ni$: C, 65.9%; H, 6.63%; N, 7.68%. Found: C, 62.0%; H, 6.94%; N, 7.24%. Multiple attempts using microcrystalline samples to obtain satisfactory %C analyses yielded reproducibly low values consistent with incomplete combustion.

$[Bu_4N]_2[trans\text{-}(Ph_2Bt)_2NiBr_2]$. $[Ph_2Bt]_2Ni$ (200 mg, 0.32 mmol) was added to 20 mL of ethylene glycol dimethyl ether (DME). To the suspended solution was added $[Bu_4N]Br$ (205 mg, 0.63 mmol) slowly. The reaction mixture was stirred for 12 h resulting in a color change of the suspension from red to yellow-green. The yellow-green solid was collected by filtration. The product, $[Bu_4N]_2$-[*trans*-$(Ph_2Bt)_2NiBr_2$], was isolated as yellow-green crystals by diffusing ether into its concentrated acetone solution. Crystalline yield: 176 mg (43%). UV−vis (acetone) λ_{max} (ϵ, $M^{-1}cm^{-1}$): 360 nm (3800), 558 nm (130), 662 nm (60), 962 nm (100). Anal. Calcd for $C_{64}H_{112}B_2Br_2N_2S_4Ni$: C, 60.2; H, 8.83; N, 2.19. Found: C, 60.2; H, 9.14; N, 2.17. $\mu_{eff} = 2.6\ \mu_B$ in acetone.

$[Bu_4N]_2[cis\text{-}(Ph_2Bt)_2Ni(NCS)_2]$. $[Ph_2Bt]_2Ni$ (200 mg, 0.32 mmol) was added to 20 mL of CH_3CN. To the suspended solution was added $[Bu_4N]SCN$ (950 mg, 3.2 mmol), slowly resulting in a homogeneous green solution. The green solution was stirred for 4 h. The solvent was removed in vacuo. The remaining green oil was dissolved into 10 mL of ethanol and filtered. Slow evaporation afforded blue crystals. Crystalline yield: 234 mg (68%). UV−vis (CH_3NO_2) λ_{max} (ϵ, M^{-1} cm^{-1}): 340 nm (4000), 625 nm (120), 990 nm (100). Anal. Calcd for $C_{66}H_{112}B_2N_4S_6Ni$: C, 64.2; H, 9.15; N, 4.54. Found: C, 61.1; H, 9.35; N, 4.57. Multiple attempts using crystalline samples to obtain satisfactory %C analyses yielded reproducibly low values consistent with incomplete combustion. $\mu_{eff} = 2.7\ \mu_B$ in CD_3NO_2. FT-IR (KBr): $\nu_{CN} = 2090$, 2084 cm^{-1}.

Variable Temperature ^1H NMR Studies of $[Ph_2Bt]_2Ni$. Proton NMR spectra of $[Ph_2Bt]_2Ni$ were recorded in CD_2Cl_2 from 203 to 303 K in 10 K intervals. To determine the exchange rate constant, *k*, the following expressions were used in (i) the stopped exchange limit, $\Delta\nu = k/\pi$; (ii) the intermediate exchange regime, $k = 2.2\delta\nu$; (iii) the fast exchange regime, $\Delta\nu = \pi(\delta\nu)^2/2k$ with $\Delta\nu$ = line width and $\delta\nu$ = the chemical shift difference of exchange sites. The rate constants were fit to the Arrhenius expression (ln *k* against $1/T$) yielding the activation energy, E_a.

Crystallographic Structural Determinations. Suitable air-stable crystals were selected and mounted on thin glass fibers using epoxy. Air-sensitive crystals were handled under an inert atmosphere and sealed in thin walled capillary tubes. Preliminary unit cell determinations were obtained by harvesting reflections from three orthogonal sets of 15 frames, using 0.3° ω scans. These results were confirmed by refinement of unit-cell parameters during integration. The unit cell for $[Ph_2Bt]_2Ni$ was determined using least squares refinement of 25 reflections with $2° \le 2\theta \le 25°$. Crystallographic information is summarized in Table 1. All structures were solved using direct methods. Non-hydrogen atoms were located by difference Fourier synthesis and were refined anisotropically. Hydrogen atoms were added at calculated positions and treated as isotropic contributions with thermal parameters defined as 1.2 or 1.5 times that of the parent atom. All software and sources of scattering factors are contained in SHELXTL program library (version 5.10, G. Sheldrick, Bruker-AXS, Madison, WI.)

The systematic absences in diffraction data for $[Ph_2Bt]_2Ni$, $[Ph_2Bt^{tBu}]Ni(\eta^2\text{-}CH_2SBu^t)$, $[Bu_4N]_2[trans\text{-}(Ph_2Bt)_2NiBr_2]$, and $[Bu_4N]_2$-$[cis\text{-}(Ph_2Bt)_2Ni(NCS)_2]$ were consistent with the reported space groups. The *E*-statistics for $[Bu_4N]_2[trans\text{-}(Ph_2Bt)_2NiBr_2]$ suggested a noncentrosymmetric space group. The correct absolute structure was unambiguously determined; Flack parameter = 0.00(6). $[Bu_4N]_2[cis\text{-}(Ph_2Bt)_2Ni(NCS)_2]$ cocrystallizes with one molecule of acetonitrile in the lattice. The structure of $[Ph_2Bt]_2Ni$ was communicated previously. The crystallographic data are included in Table 1 for comparison. The ligand $Bu_4N[Ph_2Bt]$ has been structurally characterized. A thermal ellipsoid plot and crystallographic tables are included as Supporting Information.

Acknowledgment. We thank Julie Dupont for the preparation and electrochemical characterization of $[Bp^*]_2Ni$. We gratefully acknowledge the financial support provided by the National Science Foundation (NYI and CHE-9974628 to C.G.R.).

Supporting Information Available: Crystallographic data in CIF format. This material is available free of charge via the Internet at http://pubs.acs.org.

IC010966R